4
Optimization of black chrome as a spectrally selective coating for radiation calorimeter (RADCAL)

4.1 Introduction

A selective solar absorber is required to extract the maximum heat from incoming solar radiation after reflection from silver-coated reflecting layer in radiation calorimeter (RADCAL) [Verma et al., 2018]. The radiation calorimeter is a device to evaluate the local concentrated solar irradiance (CSI) incident on the surface of a receiver. It is necessary to assess the performance of a concentrated solar thermal system using, for example, a volumetric receiver for applications. It is designed as a cavity based on the black body concept to maximize the absorption of the incident CSI on its absorbent surfaces. The energy absorption causes an increase in the temperature of RADCAL, which is controlled by an external water jacket to limit its value to 100 °C for reducing the use of pressurized water. At any time and possibly in a state of equilibrium, the CSI is estimated according to the principle of energy conservation. The radiation calorimeter (RADCAL) consists of a reflector and absorbing surfaces, **Figure 4.1,** where the incident concentrated solar irradiance (CSI) should be reflected without any loss onto the absorber surface. The absorber surface is water-cooled simultaneously to measure the thermal equivalent of the incident irradiance, thus finally the equivalent sun concentration. The solar selective coating is deposited on its absorber surface and characterized using standard methodologies. The reflector surface coated with silver thin metallic film, and the same has been discussed in detail in the Appendix at the end of this chapter. The desired absorbance in the UV-Vis-NIR range (0.3 - 2.5 µm) is ≥ 0.95, and it is also necessary that the thermal emittance in the IR range (2.5 - 25 µm) is ≤ 0.05 [Kennedy et al., 2002]. Ceramic-metal (cermet) composite structures usually show high absorptance in low wavelength range and low emittance in the high wavelength range. The fabrication of cermet composite structure is also relatively easy and can be prepared using several methods, such as physical and chemical deposition processes. The electrochemical deposition process is quite promising because of its simple experimental requirements and uniform film depositions. Absorber coating with air and thermal stability till ca. 200 °C is required for RADCAL. The black chrome coating is usually stable up to 250 ° C, thus, suitable for the absorbent material in RADCAL for a high absorption capacity in a spectral region of 0.3 to 3 µm [Cao et al., 2014, McDonald, 1975b, Bogaerts & Lampert, 1983] and low emittance for thermal radiation exceeding 3 µm. The deposition conditions need to optimize for deposition on arbitrary surfaces, e.g., curved surfaces, to realize the uniform deposition.

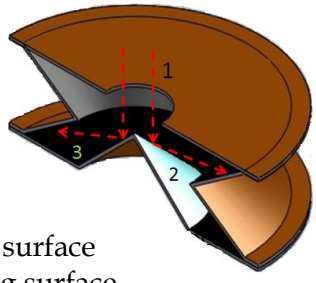

1 Rays
2 Reflector surface
3 Absorbing surface

Figure 4.1 3 D view of radiation calorimeter (RADCAL) showing reflector (2) and absorbing surface (3) [Verma et al., 2018].

4.2 Experimental detail

Black chrome as a solar absorber is coated on the absorber part of the radiation calorimeter using electrodeposition. Before depositing RADCAL absorber part, black chrome electrodeposition conditions are optimized for large surfaces, comparable to the RADCAL surfaces. Ni as IR reflector also electrochemically deposited on absorber surface before black chrome deposition. The detailed electrodeposition condition is discussed in **section 3.2.1.2.**

4.3 Results and Discussion

The selective absorber coating in RADCAL comprises of a nickel layer as an IR reflective layer, followed by the BC (Cr-Cr_2O_3) layer as an absorbing layer. The electrochemical deposition is used for the deposition of these layers. The bath conditions for Ni and BC are summarized in subsection 3.2.1.2 of chapter 3. The details of optimized conditions for Ni infrared reflector are summarized in **Table 3.1** and the respective mechanism in **Table 3.2** together with the deposition scheme in **Figure 3.2.** In brief, a thin nickel-metal film is deposited by adjusting a constant current density J = 850 A / m^2 to an electrode separation of ~ 30 mm for different durations. Nickel films are deposited for 30, 60, and 120 seconds and the thickness of the nickel layer for different deposition times is measured using a thickness profilometer. The variation in the thickness of the nickel layer as a function of deposition time is summarized in **Figure 4.2 (a)**. The mass of nickel deposited on the substrate is calculated by Faraday's laws and using equations (4.1) [Jensen, 2012, Paunovic et al., 2010].

$$W = \frac{ItM}{nF} \tag{4.1}$$

where W, I, t, M, n, and F (~ 96500 C mol^{-1}) denote electrodeposited weight, current, time, the molecular weight of the deposited atom or molecule, number of moles of electrons and Faraday constant respectively. The calculated weight of deposited nickel is approximately 0.080 g for a 30-second electrodeposited thin film, while the measured weight is approximately 0.05 g. The observed difference in calculated and lower measured weight is attributed to the lower electrode efficiency (ε_f), defined as (equation 4.2)

$$\varepsilon_f = \frac{W_a}{W_{th}} \times 100 \tag{4.2}$$

where W_a and W_{th} are the actual and theoretical weight of deposited material.

The estimated yield of nickel electrodes is approximately 63% ± 9%. Considering the relative error bars, the minimum and maximum electrode efficiency values are ~ 54% and 72%, respectively. These limiting cases for thickness, as well as the current electrode yields, are summarized in **Figure 4.2** for thin electrodeposited nickel films. The measured thicknesses of a thin infrared reflector nickel films are ~ 1, 1.8, and 2.4 µm for 30, 60, and 120 seconds depositions (data square, **Figure 4.2**), respectively. The optical properties of these thin films are analyzed with an FTIR spectrometer in 2.5 to 25 µm, and the measured spectral reflectance is used to estimate the emissivity values of nickel films. The emissivity values for the nickel reflective layers are summarized in **Figure 4.2(b)** for different thicknesses. The high reflectivity between 2.5 and 25 µm can be noticed, and the calculated emissivity values are ≤ 0.03. Therefore, a micrometer thick IR nickel film reflector is used together with a black chrome absorbing layer for the selective spectral coating response for the RADCAL absorbing surface.

The deposition of the black chrome layer is optimized for spectral absorption after the deposition of a micron thick Ni layer as an infrared reflector on copper substrates. The

electrochemical deposition process was used for the deposition of the black chrome absorbing layer, and the deposition process is described in the experimental section with the bath conditions and the probable deposition reaction mechanisms in **Tables 3.1** and **3.2,** respectively, together with deposition scheme in **Figure 3.2**. For black chrome deposition, the current density and deposition time are varied for 0.0035 A cm^{-2} current density. The respective thicknesses measured for the deposition parameter time and current density are summarized in **Figures 4.3(a & b)**.

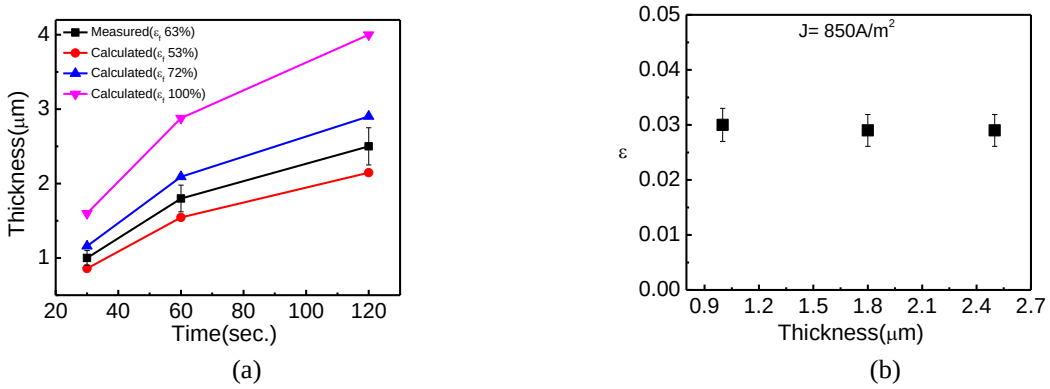

Figure 4.2 (a) Thickness with time graph (b) Emissivity with thickness graph of Ni/Cu structure

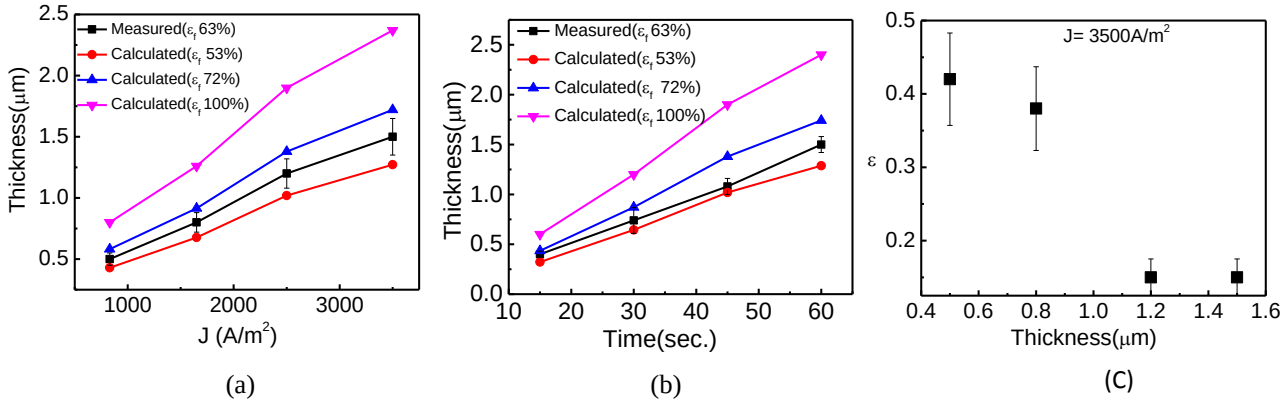

Figure 4.3 (a) Thickness with current density (b) Thickness with time and (c) Emissivity with thickness graph for BC/Ni/Cu structures

The weight of the deposited BC is calculated using equation (4.1) and is found to be 0.766 g for a 60 s electrodeposited thin film. However, the measured weight of electrolytic BC is 0.478 g for the same BC thin film. The difference in the calculated and measured weight of the black chrome film is due to the lower electrode yields. A similar phenomenon had already been observed in the case of electrochemical deposition of thin nickel films. The respective thicknesses with the limits (the minimum and the maximum) and the current performances of the electrodes are presented in the respective figures, together with the case of 100% yield for the electrodes for comparison. The observed increase in thickness is consistent in all these estimates with the measured thickness and the values calculated with the actual electrode yields are very close to the measured thicknesses. The reflectance of black chrome deposited on the Ni / Cu structures is recorded using the FTIR spectroscopy measurements and the emittance is calculated using the spectral reflectivity data. It is summarized in **Figure 4.3(c)** for BC / Ni / Cu structures with different thicknesses of BC absorbent layer. The emissivity values are higher for the lower thicknesses for BC thin films. The emissivity decreases rapidly with increasing BC thickness, either increasing the current density or increasing the deposition time. A higher emissivity value for the thickness of the black chrome ≤ 1 μm is attributed to a lower fraction of chromium metal in a ceramic chromium oxide matrix, which plays a crucial role in obtaining the

desired optical and thermal response. Therefore, a thin black chrome film with a thickness of 1.5 µm is chosen to cover the RADCAL absorbing surface. A thin nickel and black chrome films with optimized thicknesses ~ 1 and 1.5 µm, respectively, are used to cover the actual RADCAL absorbing surface. **Figure 4.4** shows camera images of the deposited RADCAL absorbent surface.

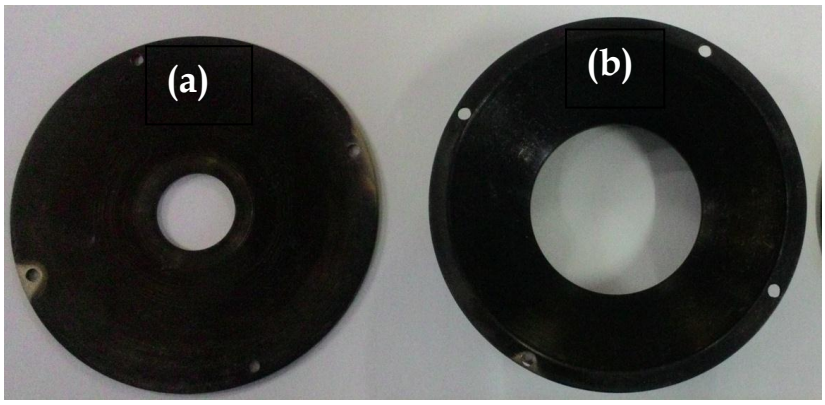

Figure 4.4 (a & b) Optical image of absorber surface coated with black chrome coating

The different structural, microstructural, and surface morphological measurements are carried out for fabricated black chrome structure to understand the evolution of its structure and optical properties. XRD measurements are carried out to investigate its crystallographic information. **Figure 4.5** shows the XRD plot for fabricated BC/NI/Cu samples. The observed peaks at 2θ = 43.4, 50.4, and 74 ° correspond to (111), (200) and (220) diffraction peaks for Cu substrate. The diffraction peaks at 2θ = 44.7 and 51.8˚ correspond (111) and (200) chromium metal planes. The chromium oxide phase was not observed in the XRD spectrum, suggesting the presence of oxide in the amorphous phase. It may be advantageous because of no finite grains, and thus, minimizing the sites of active interaction near the grain boundaries for air and gas pollutants, and protecting against corrosive environmental degradation. **Figure 4.6** shows the optical image of nickel-coated copper (Ni/Cu), and black chrome coated on nickel-coated copper (BC/Ni/Cu) top surfaces. The smooth and bright surface was observed in the optical image (**Figure 4.6(b)**). However, substrate surface imprints are visible in SEM images. The granular structure for Ni thin film is observed, however randomly oriented grains and rough terrains were observed for black chrome (BC) surfaces. The inset image in **Figure 4.6(b & c**) shows EDX measurements. EDX studies suggest the metallic nature of fabricated Ni/Cu structures acting as IR reflecting layer and Cr metal-rich fabricated black chrome structure. **Figures 4.6 (e & f)** show the 3-D topographical images of fabricated Ni/Cu and BC/Ni/Cu thin film. The surface imprints are visible in both the images. The measured surface roughness (RMS) for fabricated Ni/Cu layer was nearly half ~ 16.90 nm compared to that of Cu substrate ~ 32nm, which is due to the uniform growth of Ni layer. However, for BC / Ni / Cu layer, the increase in surface roughness was observed, which is ~ 21.05 nm. This is attributed to hillock-like film growth in the case of BC deposition, as can be seen in **Figures 4.6 (e & f)**. The measured thicknesses for Ni and BC films are approximately 1 ± 0.11 µm and 1.5 ± 0.031 µm, respectively. The UV-Vis and FTIR optical reflectance measurements were performed for optical properties estimation.

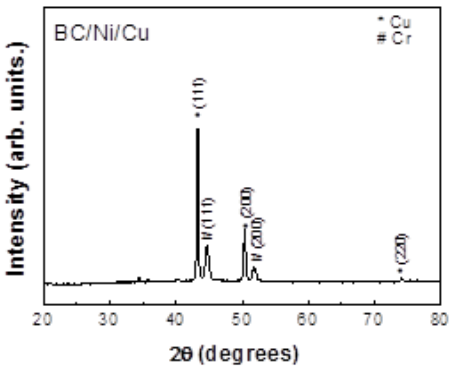

Figure 4.5 The XRD plot of deposited BC/Ni/Cu structure

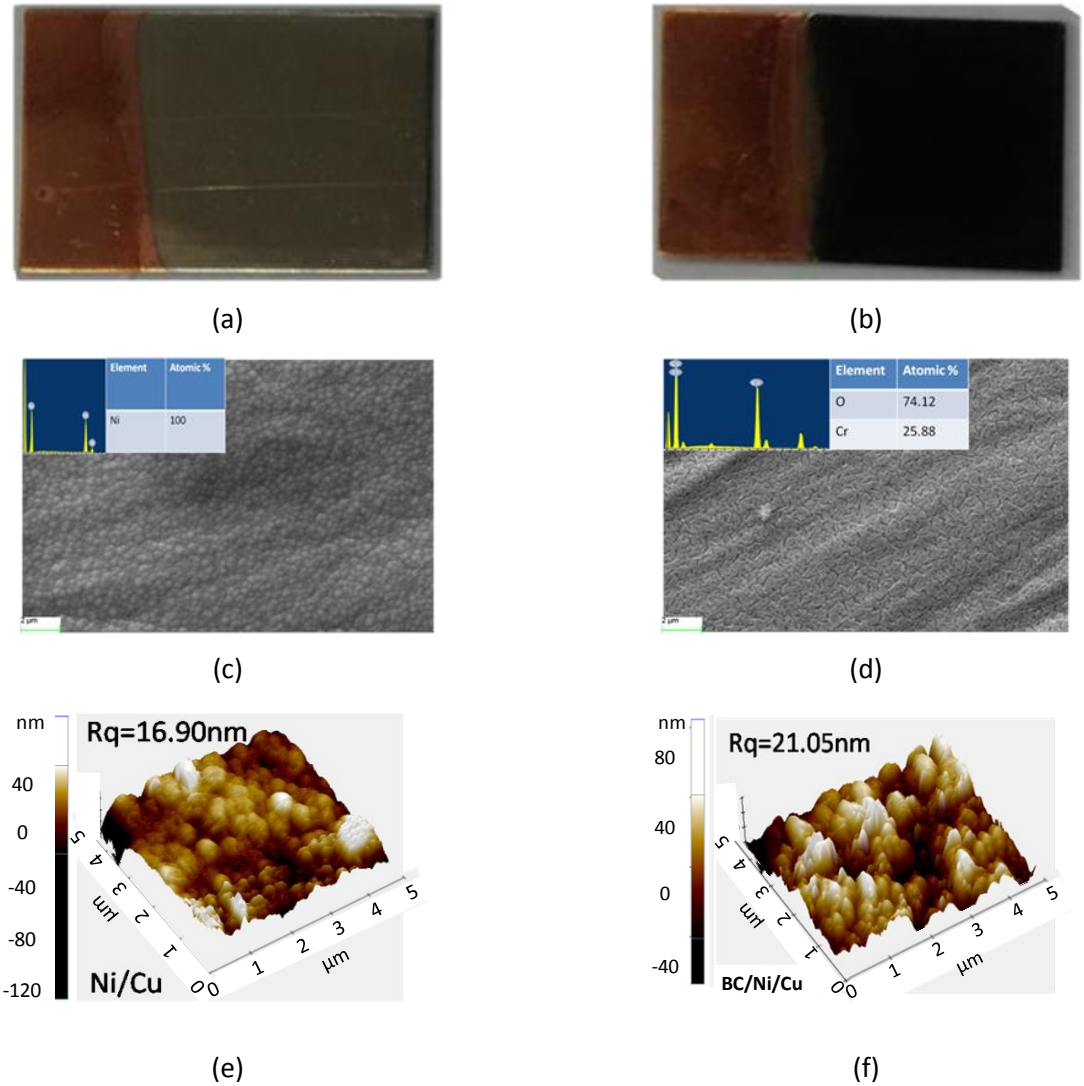

Figure 4.6 (a, b) Optical image (c, d) SEM image (e, f) 3- D topographic image of Ni/Cu and BC/Cu/N structure

Figures 4.7 (a, c & d) present the measured reflectance in UV-Vis and IR range for different BC / Ni / Cu coated samples fabricated under identical deposition conditions. The measured reflectance of the non-optimized sample is also included for comparison. The measured reflectance is used for computing absorptance and emittance values. The calculated absorptance using equation (1.4) for the optimized sample was ≥ 0.95 ± 0.01. Inset images of **Figure 4.7 (a, c & d)** are showing the measured reflectance**.** The calculated emittance using equation 2.4 is ≤ 0.14 ± 0.02 in 2.5-25 μm range for the optimized structure. In case of composite

matrix containing large metal volume fraction, the effective dielectric constant of the composite matrix is generally calculated using Bruggeman model of effective medium theory approach using equation (4.3) [Nikalasson et al., 1981]

$$0 = f_A \frac{\varepsilon_A - \varepsilon}{\varepsilon_A + 2\varepsilon} + f_A \frac{\varepsilon_B - \varepsilon}{\varepsilon_B + 2\varepsilon} \quad 4.3$$

where ε is the effective dielectric constant of the composite medium at a given wavelength, ε_A is metal-dielectric constant, and ε_B is the dielectric constants of the pristine dielectric medium, f_A is the metallic volume fraction in a metal-dielectric matrix and $f_B = 1 - f_A$.

Further, composite matrix optical constant N can be calculated as $\varepsilon = N^2$, where N = n – ik; n and k are refractive index and extinction coefficient, respectively. For normal incidence, adopting a matrix approach for the multi-layered system [Verma et al., 2018] is:

$$\begin{bmatrix} \alpha \\ \beta \end{bmatrix} = \prod_{j=1}^{m} \begin{bmatrix} \cos\delta_j & \frac{i}{N_j}\sin\delta_j \\ iN_j \sin\delta_j & \cos\delta_j \end{bmatrix} \begin{bmatrix} 1 \\ N_{m+1} \end{bmatrix} \quad 4.4$$

Here $i^2 = -1$, N_j represents jth layer optical constant and $\delta_j = \frac{2\pi}{\lambda} N_j d_j$ (for normal incidence) represent phase thickness for the j^{th} layer. The refractive index of the multilayer with a substrate is denoted by β/α. Multilayer system's reflectance (R) can be calculated as

$$R = \left(\frac{N_o - \beta/\alpha}{N_o + \beta/\alpha} \right) \left(\frac{N_o - \beta/\alpha}{N_o + \beta/\alpha} \right)^* \quad 4.5$$

Where N_0 (=1) is air optical constant

The optical constants for Cu, Ni, Cr, and Cr_2O_3 materials are borrowed from the literature [Rakić et al., 1998, Werner et al., 2009, Ordal et al., 1987, Babar & Weaver, 2015, Ordal et al., 1985] and used to compute reflectance (R) for BC coated on Ni coated substrate. The calculated reflectance is in accordance with the measured reflectance for the BC / Ni / Cu sample **(Figure 4.7 (a))** in the IR range for the 0.46 metal fractions present in BC. However, the calculated reflectance is not matching with the measured reflectance in the lower wavelength region. It is attributed to the non-availability of high-quality optical data in the lower wavelength range. Also, the effect of surface irregularities and the interface is not included in effective medium approach while simulating the multilayer structures.

The impact of heat treatment on the selective coating is essential to understand the stability of the coatings and the device under normal operating conditions, in addition to its optical performance. The cyclic heating of the BC / Ni / Cu structure is performed in an oven under a controlled temperature environment by varying from room temperature to 200 ° C at a heating rate of 0.16 ° C / sec, followed by natural sample cooling to the room temperature. The samples are subjected to periodic heating cycles for approximately 35 hours, as shown in **Figure 4.7 (b)**. The measured IR reflectance of the samples after periodic heating in a wavelength range of 2.5 to 25 μm is illustrated in **Figure 4.7 (c)** with an inset image representing the UV-Vis reflectance of the samples. The reflectance curves do not show significant change after periodic heating cycles throughout the entire thermal wavelength region, indicating that the deposited black chrome structures are thermally robust. **Figure 4.7 (d)** summarizes the reflectance for BC / Ni / Cu structures for as prepared, and heat-treated samples. The emissivity was also calculated

after periodic heat-treatment and was found to be approximately 0.17, similar to the emissivity of the as prepared samples. A similar absorptance value indicates that the cladding structures are thermally stable.

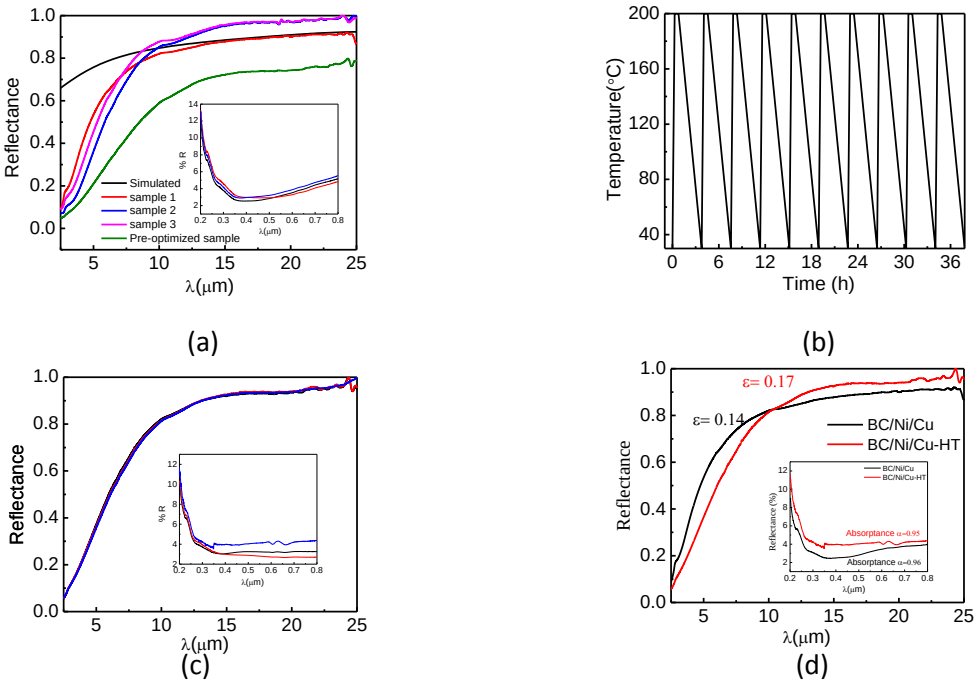

Figure 4.7 (a) Reflectance versus wavelength plot of BC on nickel coated Cu substrate (b) heating cycle schematic (c) Reflectance versus wavelength plot of BC/Ni/Cu-HT (d) Reflectance versus wavelength plot of BC/Ni/Cu and BC/Ni/Cu-HT.

4.4 Conclusion

The experimental deposition conditions were optimized and analyzed to get optimal optical properties for BC absorber together with Ni as an infrared reflector. The absorptance and emittance of the optimized BC/Ni/Cu structures are 0.95 and 0.14, respectively. The coated structure shows thermal stability in the medium temperature range. Further, the adopted process is scalable for the deposition of BC coatings on a large area of arbitrary geometrical shapes.